Magnetospirillum magneticum as a living iron chelator induces transferrin receptor 1 upregulation in cancer cells

Stefano Menghini†, Ping Shu Ho†, Tinotenda Gwisai, Simone Schuerle*

Institute for Translational Medicine, Department of Health Sciences and Technology, ETH Zurich, CH-8092 Zurich, Switzerland.

† **These authors contributed equally**
***Correspondence:**
Corresponding Author
simone.schuerle@hest.ethz.ch

Keywords: Magnetotactic bacteria, iron chelators, cancer therapy, transferrin receptor 1, siderophores

Abstract

Interest has grown in harnessing biological agents for cancer treatment as dynamic and responsive vectors with enhanced tumor targeting. While bacterial traits such as proliferation in tumors, modulation of an immune response, and local secretion of toxins have been well studied, less is known about bacteria as competitors for nutrients. Here, we investigated the use of a bacterial strain as a living iron chelator, competing for this nutrient vital to tumor growth and progression. We established an *in vitro* co-culture system consisting of the magnetotactic strain *Magnetospirillum magneticum* AMB-1 incubated under hypoxic conditions with human melanoma cells. Siderophores produced by 10^8 AMB-1/mL in human transferrin (Tf)-supplemented media were found to alter the Tf structure with an effect equivalent to 3.78 µM ± 0.117 µM deferoxamine, a potent drug used in iron chelation therapy. Our experiments revealed an increased expression of transferrin receptor 1 (TfR1), indicating the bacteria's ability to influence iron homeostasis in human melanoma cells. Our results show the potential of a bacterial strain as a self-replicating iron-chelating agent, which could serve as an additional mechanism reinforcing current bacterial cancer therapies.

1. Introduction

Due to limited selectivity in systemically delivered cancer therapeutics, interest has grown in harnessing bacteria as living, tumor-targeting anticancer agents. The therapeutic potential of facultative anaerobic bacteria has been supported by studies demonstrating the delivery of non-pathogenic strains of *Escherichia coli* to solid flank tumors with associated tumor regression. Additionally, safe administration of *Salmonella typhimurium* (VPN20009) has been shown for animal models and patients with metastatic melanoma (Chowdhury et al., 2019, Clairmont et al., 2000, Toso et al., 2002). Bacteria can act therapeutically by secreting innate or engineered toxins in situ (e.g. hemolysin E), transporting attached nanodrug formulations, or stimulating an immune response (Duong et al., 2019, Sedighi et al., 2019, Din et al., 2016, Harimoto et al., 2019). Colonizing bacteria can also engage in nutrient competition within the tumor microenvironment (Forbes, 2010, Sznol et al., 2000, Song et al., 2018). While the starvation of glucose as a crucial energy source to all cells has been studied intensively (Grasmann et al., 2019, Vander Heiden et al., 2009, Pavlova and Thompson, 2016), other nutrients that are in specifically high demand by cancer cells might serve as more specific, vulnerable targets for deprivation.

For example, iron metabolism is significantly altered in mammalian tumor cells and recognized as a metabolic hallmark of cancer (Wang et al., 2018, Torti and Torti, 2013). The main iron uptake mechanism adopted by most cells utilizes the internalization of transferrin receptor 1 (TfR1) upon binding of iron-bound transferrin (Tf). TfR1 expression positively correlates with cellular iron starvation and is upregulated in cancer cells, since malignant cells generally require a nutrient surplus (Torti and Torti, 2013, Lane et al., 2015, Steegmann-Olmedillas, 2011). Accordingly, several types of iron scavenging molecules have been utilized to compete with malignant cells for available iron sources and have demonstrated significant anti-neoplastic activity both, *in vitro* and *in vivo* (Bedford et al., 2013, Ford et al., 2013, Lui et al., 2013) Promising bacteria-derived iron-chelating siderophores, such as deferoxamine (DFO), as well as synthetic iron chelators have been developed for therapeutic purposes (Hatcher et al., 2009). However, non-negligible side effects, including systemic toxicity and low efficacy, have hampered their translation into clinical trials as therapeutic agents for cancer treatment (Richardson, 2002, Yu et al., 2012b, Saha et al., 2019).

Here we investigate the potential of a specific bacterial strain with high demand for iron to serve as local, self-replicating iron chelator that could thereby reduce systemic effects. Magnetotactic bacteria, like other bacteria, possess the ability to secrete iron-scavenging siderophores. Unlike other bacteria, their demand for iron is particularly high, since this mineral is crucial both for their survival and synthesis of unique intracellular organelles called magnetosomes. (Mirabello et al., 2016, Faivre and Schüler, 2008). These biomineralized magnetic nanocrystals are arranged in chains enclosed in a lipid bilayer and enable the bacteria to align with magnetic fields (Bazylinski and Williams, 1970, Yan et al., 2012, González et al., 2015). Furthermore, MTB are aerotactic, possessing an oxygen-sensing system that regulates motility in an oxygen gradient (Lefèvre et al., 2014). These features have previously been leveraged to magnetically guide MTB to the hypoxic core of solid tumors, yielding significantly higher tumor accumulation and penetration compared to their administration in the absence of external magnetic fields (Felfoul et al., 2016). Once on site, nutrients from the tumor microenvironment are sourced to maintain proliferation and growth, and we hypothesize that MTB could induce iron deprivation of cancer cells.

To study this, we employed *Magnetospirillum magneticum* strain AMB-1 and first quantified the production of siderophores, benchmarked with molar concentrations of DFO. We then investigated the influence of AMB-1 on cell surface TfR1 expression using human melanoma cells and demonstrated the ability of AMB-1 to affect iron homeostasis. The iron scavenging capabilities of bacterial strains with naturally high or enhanced siderophore production may act as an additional mechanism for bacterial cancer therapy, complementing or augmenting established bacterial anticancer mechanisms.

2. Materials and Methods

2.1. Bacterial strain and culture condition

Magnetospirillum magneticum AMB-1, a strain of magnetotactic bacteria, was purchased from ATCC (ATCC, Manassas, Virginia, USA). AMB-1 bacteria were grown anaerobically at 30°C, passaged weekly and cultured in liquid growth medium (ATCC medium: 1653 Revised Magnetic Spirillum Growth Medium). *Magnetospirillum magneticum* Growth Media (MSGM) contained the following per liter: 5.0 mL Wolfe's mineral solution (ATCC, Manassas, Virginia, USA), 0.45 mL Resazurin, 0.68 g of monopotassium phosphate, 0.12 g of sodium nitrate, 0.035 g of ascorbic acid, 0.37 g of tartaric acid, 0.37 g of succinic acid and 0.05 sodium acetate. The pH of the media was adjusted to 6.75 with sodium hydroxide (NaOH) and then sterilized by autoclaving at 121°C. 10 mM ferric quinate (200x) Wolfe's Vitamin Solution (100x) (ATCC, Manassas, Virginia, USA) were added to the culture media shortly before use. The concentration of AMB-1 in solution was determined by optical density measurement (Spark, Tecan, Männedorf, Switzerland) and the approximate number of bacteria was extrapolated from a standard curve.

2.2. CAS assay to asses siderophore quantification

Magnetospirillum magneticum AMB-1 were cultured in 1.7 mL phenol red-free DMEM (11054020, Invitrogen, Carlsbad, California, USA) supplemented with GlutaMAX (35050061, Invitrogen, Carlsbad, California, USA) in a sealed 1.5 mL Eppendorf tube at 37°C for 24 h. FBS was excluded from the media and replaced with a known concentration of iron source; 25 µM holo-transferrin (T0665, Sigma-Aldrich, St. Louis, Missouri, USA). Quantification of siderophores produced by AMB-1 was performed using the Chrome Azurol S (CAS) assay (199532, Sigma-Aldrich, St. Louis, Missouri, USA) (Schwyn and Neilands, 1987). 100 µL of each sample's supernatant was collected and mixed with 100 µL CAS assay solution on a transparent 96-well plate. The assay was then incubated in the dark at room temperature for 1 h before the absorbance was measured at 630 nm on a multimode microplate reader (Spark, Tecan, Männedorf, Switzerland). The measurement was expressed in siderophore production unit (s.p.u.), which was calculated as follows:

$$\text{Siderophore production unit (s. p. u.)} = \frac{\text{OD}_{630,\text{ref}} - \text{OD}_{630}}{\text{OD}_{630,\text{ref}}}$$

DMEM supplemented with different concentrations of deferoxamine mesylate salt (DFO, D9533, Sigma-Aldrich, St. Louis, Missouri, USA) was prepared by serial dilution and used to generate a calibration curve (Supplementary 1).

2.3. Analysis of human transferrin using SDS-PAGE Electrophoresis

AMB-1 bacteria (1 x 10^8 cells/mL) were cultured in 1.7 mL phenol red-free DMEM (11054020, Invitrogen, Carlsbad, California, USA) in a sealed 1.5 mL Eppendorf tube at 30°C

for 48 h. Excess volume was used to ensure no or minimal air was trapped in the tubes. 25 µM holo-transferrin (holo-Tf, T4132, Sigma-Aldrich, St. Louis, Missouri, USA), or 25 µM apo-transferrin (apo-Tf, T2036, Sigma-Aldrich, St. Louis, Missouri, USA) respectively were added to the mammalian cell culture media. Changes in transferrin molecular mass during the growth of AMB-1 were evaluated by sodium dodecyl sulfate-polyacrylamide gel electrophoresis (SDS-PAGE) analysis of culture supernatant. Electrophoresis was conducted using the protocol described by Laemmli (Laemmli, 1970) and protein loading of each sample was normalized to 2 µg. Proteins were visualized using SYPRO ruby protein stain (1703126, Bio-rad, Hercules, California, USA). The electrophoresis chamber and the reagents were purchased from Bio-rad. Stained gels were imaged using a fluorescent scanner (Sapphire Biomolecular Imager, Azure Biosystems, Dublin, California, USA) at 488 nm excitation and 658 nm emission.

2.4. Mammalian cell culture

Human melanoma MDA-MB-435S cells (ATCC, Manassas, Virginia, USA) were cultured in high glucose Dulbecco's Modified Eagle's Medium (DMEM, Invitrogen, Carlsbad, California, USA) supplemented with 10% fetal bovine serum (FBS, Biowest, Nuaille, France) and 1% penicillin-streptomycin (CellGro, Corning, New York, USA). All cells were incubated at 37°C in a humidified atmosphere with 5% CO_2 at 37°C.

2.5. Co-culture of mammalian cancer cells with magnetotactic bacteria

Human melanoma MDA-MB-435 cells (1 x 10^5 cells) were cultured on 12-well plates and incubated in a 5% CO_2 incubator at 37°C for 24 h. For microscopic analysis at high magnification (> 40x), a circular cover slip was placed in each well prior to cell seeding. Following incubation, *Magnetospirillum magneticum* AMB-1 (1 x 10^6 – 1 x 10^8 cells) were introduced into the wells. The well plate was stored in a sealable bag and the bag was flushed with nitrogen for 15 min in order to produce hypoxic conditions. The setup with the 12-well plate was then incubated at 37°C for 48 h. To serve as negative and positive controls, 0, 10 µM and 25 µM of the iron-chelating agent deferoxamine mesylate (D9533, Sigma-Aldrich, St. Louis, Missouri, USA) was added to the MDA-MB-435S cell culture in place of AMB-1 bacteria.

2.6. Immunofluorescence labelling of MDA-MB-435S cells

After the co-culture, cells were washed with ice cold 1X Dulbecco's Phosphate-Buffered Saline solution (DPBS, Gibco, Carlsbad, California, USA) and then blocked with a 1% Bovine Serum Albumin (BSA, Sigma-Aldrich, St. Louis, Missouri, USA) solution diluted in 1X DPBS. The cells were then incubated with 10 µg/mL primary anti-TfR1 antibody (ab84036, Abcam, Cambridge, UK) on ice in dark for one h. Subsequently, the cells were washed with ice-cold DPBS and incubated with 20 µg/mL secondary goat anti-rabbit antibody (ab150077, Abcam, Cambridge, UK) and 25 µg/mL Hoechst 33342 (H3570, Thermo Fisher Scientific, Waltham, Massachusetts, USA) on ice in dark for another hour. Next, the cells were washed with ice-cold 1X PBS twice and fixed with a 2% paraformaldehyde (PFA) solution. Fixed cells were washed three times with 1X DPBS and the cover slips were mounted on glass slides and stored overnight in dark at 4°C. A Nikon Eclipse Ti2 microscope equipped with a Yokogawa CSU-W1 Confocal Scanner Unit and Hamamatsu C13440-20CU ORCA Flash 4.0 V3 Digital CMOS camera were used for visualization. Microscope operation and image acquisition was

performed using Nikon NIS-Elements Advanced Research 5.02 (Build 1266) software. ImageJ v2.0 (NIH) was used to process the obtained images.

2.7. Evaluation of fluorescently labelled MDA-MB-435S cells by flow cytometry

Flow cytometry was used to measure the expression of fluorescently labelled TfR1 on the surface of MDA-MB-435S cells. Cells were harvested at different timepoints during co-culture (0h, 6h, 12h, 24h) and washed in cold 1X DPBS (Gibco Carlsbad, California, USA). Harvested cells were stained with primary anti-TfR1 antibody (ab84036, Abcam, Cambridge, UK) at a concentration of 10 µg/mL. After 1 h of incubation on ice, cells were washed twice with 1X DPBS and then stained with 20 µg/mL secondary goat anti-rabbit antibody (ab150077, Abcam, Cambridge, UK). Finally, cells were washed twice with 1X DPBS and analyzed by flow cytometry with BD LSRFortessa (BD Biosciences, San Jose, California, USA) using a 488nm excitation laser and 530/30 and 690/50 band pass emission filters for detection. FlowJo™ (Tree Star) software was used to evaluate the data.

Flow cytometry was used to assess the cell membrane integrity of MDA-MB-435S cells. Cells were harvested at different timepoints during co-culture (0h, 6h, 24h) and washed in cold 1X DPBS. Collected cells were stained with 1 µg/mL Propidium Iodide (V13242, Thermo Fisher Scientific, Waltham, Massachusetts, USA) and incubated for 30 in a humidified atmosphere with 5% CO_2 at 37°C. Finally, cells were washed twice with 1X DPBS and analyzed by flow cytometry with BD LSRFortessa (BD Biosciences, San Jose, California, USA) using a 488nm excitation laser and 610/10 bandpass emission filters for detection. FlowJo™ (Tree Star) software was used to evaluate data and graphs were plotted using Prism 8.0 (GraphPad).

2.8. Statistics and data analysis

All graphs and statistical analyses were generated using Prism 8.0 (GraphPad). Statistical significance and number of replicates of the experiments are described in each figure and figure legend. Error bars, where present, indicate the standard error of the mean (SD). P values are categorized as * $P<0.05$, ** $P<0.01$, and *** $P<0.001$.

3. Results

3.1. AMB-1 produced siderophores affect human transferrin structure in mammalian cell culture medium

First, we sought to determine to what extent AMB-1 would produce siderophores in Dulbecco's Modified Eagle's medium (DMEM). Using the Chrome Azurol S (CAS) assay (Supplementary Fig. 1), 10^8 AMB-1 bacteria were found to produce 0.10 ± 0.005 siderophore units in DMEM supplemented with 25 µM holo-transferrin (holo-Tf), while siderophore production in transferrin-free DMEM was negligible (Fig. 1A). AMB-1 siderophore production was compared to the widely used iron chelator deferoxamine. It was found that the siderophores produced by 10^8 AMB-1 in Tf-supplemented media was equivalent to 3.78 µM ± 0.117 µM deferoxamine (Fig. 1B).

Having established the ability of AMB-1 to produce siderophores in Tf-supplemented media, we next determined whether AMB-1 would have an effect on human transferrin structure. SDS-PAGE analysis was used to compare DMEM supplemented with either iron-containing holo-Tf or iron-depleted apo-Tf. The apo-Tf appeared as a broader band on the SDS-gel compared to holo-Tf (Fig. 1C). Furthermore, we ascertained that holo-Tf structure was not affected by a

48 h incubation period at 30°C. To test whether the bacteria induced changes in Tf, AMB-1 were inoculated in DMEM supplemented with holo-Tf. This approach revealed that holo-Tf formed a broader band very similar to that seen for the apo-Tf band incubated in DMEM (Fig. 1C, lane 6). These experiments demonstrate that AMB-1 produced a quantifiable amount of siderophore when holo-Tf was supplemented to the mammalian cell culture media and that the structure of holo-Tf was altered by the bacteria.

3.2. AMB-1 upregulates TfR1 expression in human melanoma cells

To test whether AMB-1 can affect the iron uptake machinery in mammalian tumor cells we co-cultured AMB-1 with the human melanoma cell line MDA-MB-435S and monitored TfR1 expression using immunofluorescence. The surface expression of TfR1 increased 2.7-fold on cancer cells co-cultured with live bacteria at AMB-1:MDA-MB-435S ratios as low as 10:1 (10^6 AMB-1). The TfR1 upregulation was shown to increase with increasing bacteria ratios (Fig. 2A, B). Deferoxamine was used here to create iron-deficient cell culture conditions as a positive control. MDA-MB-435S cells showed a significant and increasing upregulation of TfR1 surface expression up to 5.6-fold. To ensure that the upregulation of TfR1 expression was on the cell surface and not cytoplasmic, cell membrane integrity in the cultures was monitored. Less than 5% of cells were stained by the cell-impermeant DNA stain propidium iodide (PI), indicating cell membrane preservation over time (Fig. 2C).

To gain insights on the TfR1 expression kinetics of the cell population, AMB-1-induced increase of cell surface TfR1 expression was analyzed over time. The effect, at an AMB-1:MDA-MB-435S ratio of 1000:1 was already apparent after 6 h of co-culture (Fig. 1D). The fluorescent intensity after 24 h of co-culture was 1.8 times higher than the initial value, while the change reached 95% of the final value after 12 h (Fig. 1E). Untreated cancer cells did not display any increase in fluorescence (Fig. 1F). Altogether, these findings show an upregulation of TfR1 on the cell surface of human melanoma cancer cells in the presence of AMB-1, thereby suggesting a direct link between AMB-1 induced disruption of iron uptake and TfR1 expression.

4. Discussion

Magnetotactic bacteria acquire iron through siderophore-mediated uptake, as ferric and ferrous ions cannot directly enter bacteria cells. We quantified the number of siderophores produced by strain *Magnetospirillum magneticum* AMB-1 and investigated the bacteria's effect on human transferrin's structure in mammalian cell culture medium. The addition of AMB-1 to the media led to a broader holo-Tf band, similar to that of apo-Tf in DMEM, suggesting that the bacteria induced changes in Tf's molecular mass and structure (Fig. 1C, lane 6). Comparing our findings to studies involving the proteolytic cleavage of transferrin by *Prevotella nigrescens* we can deduce that specific cleavage of the protein did not occur, as sub-products with lower molecular mass were not detected on the gel (Duchesne et al., 1999). Therefore, our results suggest a loss of iron ions by holo-Tf, which is consistent with bacteria-produced siderophores having a higher affinity for Fe ions compared to human transferrin (Wilson et al., 2016, Holden and Bachman, 2015). This higher affinity could be exploited by AMB-1 to efficiently compete for ferric ions with the host cells, resulting in iron starvation for the latter.

We then showed that AMB-1 inoculation with human melanoma cell cultures affects iron homeostasis of the cancer cells. Iron starvation is mainly characterized by alterations in the

iron import machinery, specifically by an upregulation of the transferrin receptor 1 on the cell surface. Increased TfR1 expression found on MDA-MB-435S melanoma cancer cells correlates with increasing bacteria ratios. This finding suggests that AMB-1 effectively competes for free iron ions and therefore limits the mineral's availability to MDA-MB-435S cells (Fig. 2A, B). Moreover, a significant increase of TfR1 expression could already be detected 6 h after inoculation (Fig. 2D-F). Similarly, the cancer cells showed a significant upregulation of TfR1 surface expression after incubation with deferoxamine (10 µM and 25 µM), in line with previous reports on cellular iron deficiency (Torti and Torti, 2013, Lane et al., 2015, Bajbouj et al., 2018). These observations demonstrated that AMB-1 affect the iron import mechanisms of human melanoma cells, acting as an effective competitor for iron when in co-culture with MDA-MB-435S cells.

Our data support the idea that AMB-1 have the ability to act as living iron chelators by secreting a quantifiable amount of siderophores. We showed that 10^8 AMB-1/mL can produce high-affinity iron scavenging molecules equivalent to 3.78 µM deferoxamine over 24 h (Fig. 1B). Previous studies demonstrated that the treatment of different cell lines with 10 µM - 30 µM deferoxamine significantly reduced cell viability *in vitro* (Ford et al., 2013, Bajbouj et al., 2018). Moreover, a significant diminution of cell viability was even detected at the lower deferoxamine concentration of 2.5 µM when combined with the chemotherapeutic drug cisplatin (Ford et al., 2013). Nonetheless, the implementation of molecular iron scavenging molecules in translational medicine is hampered by elevated systemic toxicity, as well as limited tumor selectivity. These challenges might be overcome by implementing bacteria as direct competitors for nutrients at the tumor site. The ability of AMB-1 to self-replicate and secrete comparable, sustained doses of siderophores qualifies them as promising candidates for further studies.

The intrinsic magneto-aerotactic capability of MTB allows them to regulate their motility towards environments with low oxygen concentration as well as react to externally applied magnetic fields (Lefèvre et al., 2014, González et al., 2015). Aerotaxis and hypoxic traits have also been leveraged in *Salmonella* strains, enabling them to act as bacterial anti-cancer agents that target necrotic tumor microenvironments with poor oxygen supply (Mengesha et al., 2006, Yu et al., 2012a, Kasinskas and Forbes, 2007). In addition to enhanced tumor accumulation, native bacterial cytotoxicity, expression of anticancer agents, and immunomodulation have been exploited for their use in clinical cancer therapy (Din et al., 2016, Chowdhury et al., 2019, Forbes, 2010, Duong et al., 2019). By combining iron chelation with these additional benefits of bacterial cancer therapy, we envision that MTB could become a valid therapeutic agent to implement against cancer.

Our work motivates the use of living AMB-1 as self-replicating iron scavenging organisms actively competing for this vital nutrient, with the possibility of compromising the survival of cancer cells. Further application could include the use of tumor-targeting organisms both as a monotherapy and as a combination therapy with established anti-neoplastic drugs to obtain optimal clinical outcomes. Moreover, the unique characteristics of magnetotactic bacteria could be exploited to engineer iron-scavenging strains of surrogate commensal and attenuated bacteria that have already been established as anti-cancer agents. This work lays the foundation for future investigations which combine iron chelation with bacterial cancer therapy to enhance existing therapeutic strategies and open new frontiers for combating cancer.

5. Author contributions

SS and PSH conceived and designed the experiments. PSH and SM collected and analyzed data. SM wrote the manuscript. TG assisted the authors and contributed to the paper revisions. SS supervised the study and helped writing the paper.

6. Acknowledgements

The authors thank Cameron Moshfegh for helpful discussions. Technical support was provided by the Flow Cytometry Core Facility at ETH Zurich for flow cytometry measurements. The authors appreciate the help of Nima Mirkhani with AMB-1 cultures. The authors thank Guy Riddihough (Life Science Editors) for his editing support and Michael G. Christiansen for critically reviewing the manuscript and for his assistance in creating the hypoxia device.

7. Funding

This research was supported by the Branco Weiss Fellowship-Society in Science (title: "Cancer-fighting magnetic biobots: Harnessing the power of synthetic biology and magnetism").

8. Conflict of interest

The authors declare no conflict of interest.

References

BAJBOUJ, K., SHAFARIN, J. & HAMAD, M. 2018. High-Dose Deferoxamine Treatment Disrupts Intracellular Iron Homeostasis, Reduces Growth, and Induces Apoptosis in Metastatic and Nonmetastatic Breast Cancer Cell Lines. *Technology in cancer research & treatment,* 17**,** 1533033818764470-1533033818764470.

BAZYLINSKI, D. & WILLIAMS, T. 1970. Ecophysiology of Magnetotactic Bacteria.

BEDFORD, M. R., FORD, S. J., HORNIBLOW, R. D., IQBAL, T. H. & TSELEPIS, C. 2013. Iron Chelation in the Treatment of Cancer: A New Role for Deferasirox? *The Journal of Clinical Pharmacology,* 53**,** 885-891.

CHOWDHURY, S., CASTRO, S., COKER, C., HINCHLIFFE, T. E., ARPAIA, N. & DANINO, T. 2019. Programmable bacteria induce durable tumor regression and systemic antitumor immunity. *Nature Medicine,* 25**,** 1057-1063.

CLAIRMONT, C., LEE, K. C., PIKE, J., ITTENSOHN, M., LOW, K. B., PAWELEK, J., BERMUDES, D., BRECHER, S. M., MARGITICH, D., TURNIER, J., LI, Z., LUO, X., KING, I. & ZHENG, L. M. 2000. Biodistribution and Genetic Stability of the Novel Antitumor Agent VNP20009, a Genetically Modified Strain of Salmonella typhimuvium. *The Journal of Infectious Diseases,* 181**,** 1996-2002.

DIN, M. O., DANINO, T., PRINDLE, A., SKALAK, M., SELIMKHANOV, J., ALLEN, K., JULIO, E., ATOLIA, E., TSIMRING, L. S., BHATIA, S. N. & HASTY, J. 2016. Synchronized cycles of bacterial lysis for in vivo delivery. *Nature,* 536**,** 81.

DUCHESNE, P., GRENIER, D. & MAYRAND, D. 1999. Binding and utilization of human transferrin by Prevotella nigrescens. *Infection and immunity,* 67**,** 576-580.

DUONG, M. T.-Q., QIN, Y., YOU, S.-H. & MIN, J.-J. 2019. Bacteria-cancer interactions: bacteria-based cancer therapy. *Experimental & Molecular Medicine,* 51**,** 152.

401 FAIVRE, D. & SCHÜLER, D. 2008. Magnetotactic Bacteria and Magnetosomes. *Chemical*
402 *Reviews,* 108**,** 4875-4898.
403 FELFOUL, O., MOHAMMADI, M., TAHERKHANI, S., DE LANAUZE, D., ZHONG XU, Y.,
404 LOGHIN, D., ESSA, S., JANCIK, S., HOULE, D., LAFLEUR, M., GABOURY, L.,
405 TABRIZIAN, M., KAOU, N., ATKIN, M., VUONG, T., BATIST, G., BEAUCHEMIN, N.,
406 RADZIOCH, D. & MARTEL, S. 2016. Magneto-aerotactic bacteria deliver drug-
407 containing nanoliposomes to tumour hypoxic regions. *Nature Nanotechnology,* 11**,**
408 941.
409 FORBES, N. S. 2010. Engineering the perfect (bacterial) cancer therapy. *Nature Reviews*
410 *Cancer,* 10**,** 785-794.
411 FORD, S. J., OBEIDY, P., LOVEJOY, D. B., BEDFORD, M., NICHOLS, L., CHADWICK, C.,
412 TUCKER, O., LUI, G. Y. L., KALINOWSKI, D. S., JANSSON, P. J., IQBAL, T. H.,
413 ALDERSON, D., RICHARDSON, D. R. & TSELEPIS, C. 2013. Deferasirox
414 (ICL670A) effectively inhibits oesophageal cancer growth in vitro and in vivo. *British*
415 *journal of pharmacology,* 168**,** 1316-1328.
416 GONZÁLEZ, L. M., RUDER, W. C., MITCHELL, A. P., MESSNER, W. C. & LEDUC, P. R.
417 2015. Sudden motility reversal indicates sensing of magnetic field gradients in
418 Magnetospirillum magneticum AMB-1 strain. *The ISME Journal,* 9**,** 1399-1409.
419 GRASMANN, G., SMOLLE, E., OLSCHEWSKI, H. & LEITHNER, K. 2019. Gluconeogenesis
420 in cancer cells - Repurposing of a starvation-induced metabolic pathway? *Biochimica*
421 *et biophysica acta. Reviews on cancer,* 1872**,** 24-36.
422 HARIMOTO, T., SINGER, Z. S., VELAZQUEZ, O. S., ZHANG, J., CASTRO, S.,
423 HINCHLIFFE, T. E., MATHER, W. & DANINO, T. 2019. Rapid screening of
424 engineered microbial therapies in a 3D multicellular model. *Proceedings of the*
425 *National Academy of Sciences of the United States of America,* 116**,** 9002-9007.
426 HATCHER, H. C., SINGH, R. N., TORTI, F. M. & TORTI, S. V. 2009. Synthetic and natural
427 iron chelators: therapeutic potential and clinical use. *Future medicinal chemistry,* 1**,**
428 1643-1670.
429 HOLDEN, V. I. & BACHMAN, M. A. 2015. Diverging roles of bacterial siderophores during
430 infection. *Metallomics,* 7**,** 986-995.
431 KASINSKAS, R. W. & FORBES, N. S. 2007. Salmonella typhimurium Lacking Ribose
432 Chemoreceptors Localize in Tumor Quiescence and Induce Apoptosis. *Cancer*
433 *Research,* 67**,** 3201.
434 LAEMMLI, U. K. 1970. Cleavage of Structural Proteins during the Assembly of the Head of
435 Bacteriophage T4. *Nature,* 227**,** 680-685.
436 LANE, D. J. R., MERLOT, A. M., HUANG, M. L. H., BAE, D. H., JANSSON, P. J., SAHNI, S.,
437 KALINOWSKI, D. S. & RICHARDSON, D. R. 2015. Cellular iron uptake, trafficking
438 and metabolism: Key molecules and mechanisms and their roles in disease.
439 *Biochimica et Biophysica Acta (BBA) - Molecular Cell Research,* 1853**,** 1130-1144.
440 LEFÈVRE, C. T., BENNET, M., LANDAU, L., VACH, P., PIGNOL, D., BAZYLINSKI, D. A.,
441 FRANKEL, R. B., KLUMPP, S. & FAIVRE, D. 2014. Diversity of magneto-aerotactic
442 behaviors and oxygen sensing mechanisms in cultured magnetotactic bacteria.
443 *Biophysical journal,* 107**,** 527-538.
444 LUI, G. Y. L., OBEIDY, P., FORD, S. J., TSELEPIS, C., SHARP, D. M., JANSSON, P. J.,
445 KALINOWSKI, D. S., KOVACEVIC, Z., LOVEJOY, D. B. & RICHARDSON, D. R.
446 2013. The Iron Chelator, Deferasirox, as a Novel Strategy for Cancer Treatment:
447 Oral Activity Against Human Lung Tumor Xenografts and Molecular Mechanism of
448 Action. *Molecular Pharmacology,* 83**,** 179.
449 MENGESHA, A., DUBOIS, L., LAMBIN, P., LANDUYT, W., CHIU, R. K., WOUTERS, B. G.
450 & THEYS, J. 2006. Development of a flexible and potent hypoxia-inducible promoter
451 for tumor-targeted gene expression in attenuated salmonella. *Cancer Biology &*
452 *Therapy,* 5**,** 1120-1128.
453 MIRABELLO, G., LENDERS, J. J. M. & SOMMERDIJK, N. A. J. M. 2016. Bioinspired
454 synthesis of magnetite nanoparticles. *Chemical Society Reviews,* 45**,** 5085-5106.

PAVLOVA, NATALYA N. & THOMPSON, CRAIG B. 2016. The Emerging Hallmarks of Cancer Metabolism. *Cell Metabolism,* 23**,** 27-47.

RICHARDSON, D. R. 2002. Iron chelators as therapeutic agents for the treatment of cancer. *Critical Reviews in Oncology/Hematology,* 42**,** 267-281.

SAHA, P., YEOH, B. S., XIAO, X., GOLONKA, R. M., KUMARASAMY, S. & VIJAY-KUMAR, M. 2019. Enterobactin, an iron chelating bacterial siderophore, arrests cancer cell proliferation. *Biochemical Pharmacology,* 168**,** 71-81.

SCHWYN, B. & NEILANDS, J. B. 1987. Universal chemical assay for the detection and determination of siderophores. *Analytical Biochemistry,* 160**,** 47-56.

SEDIGHI, M., ZAHEDI BIALVAEI, A., HAMBLIN, M. R., OHADI, E., ASADI, A., HALAJZADEH, M., LOHRASBI, V., MOHAMMADZADEH, N., AMIRIANI, T., KRUTOVA, M., AMINI, A. & KOUHSARI, E. 2019. Therapeutic bacteria to combat cancer; current advances, challenges, and opportunities. *Cancer medicine,* 8**,** 3167-3181.

SONG, S., VUAI, M. S. & ZHONG, M. 2018. The role of bacteria in cancer therapy - enemies in the past, but allies at present. *Infectious agents and cancer,* 13**,** 9-9.

STEEGMANN-OLMEDILLAS, J. L. 2011. The role of iron in tumour cell proliferation. *Clinical and Translational Oncology,* 13**,** 71-76.

SZNOL, M., LIN, S. L., BERMUDES, D., ZHENG, L. M. & KING, I. 2000. Use of preferentially replicating bacteria for the treatment of cancer. *The Journal of clinical investigation,* 105**,** 1027-1030.

TORTI, S. V. & TORTI, F. M. 2013. Iron and cancer: more ore to be mined. *Nature Reviews Cancer,* 13**,** 342-355.

TOSO, J. F., GILL, V. J., HWU, P., MARINCOLA, F. M., RESTIFO, N. P., SCHWARTZENTRUBER, D. J., SHERRY, R. M., TOPALIAN, S. L., YANG, J. C., STOCK, F., FREEZER, L. J., MORTON, K. E., SEIPP, C., HAWORTH, L., MAVROUKAKIS, S., WHITE, D., MACDONALD, S., MAO, J., SZNOL, M. & ROSENBERG, S. A. 2002. Phase I study of the intravenous administration of attenuated Salmonella typhimurium to patients with metastatic melanoma. *Journal of clinical oncology : official journal of the American Society of Clinical Oncology,* 20**,** 142-152.

VANDER HEIDEN, M. G., CANTLEY, L. C. & THOMPSON, C. B. 2009. Understanding the Warburg Effect: The Metabolic Requirements of Cell Proliferation. *Science,* 324**,** 1029.

WANG, Y., YU, L., DING, J. & CHEN, Y. 2018. Iron Metabolism in Cancer. *International journal of molecular sciences,* 20**,** 95.

WILSON, B. R., BOGDAN, A. R., MIYAZAWA, M., HASHIMOTO, K. & TSUJI, Y. 2016. Siderophores in Iron Metabolism: From Mechanism to Therapy Potential. *Trends in Molecular Medicine,* 22**,** 1077-1090.

YAN, L., ZHANG, S., CHEN, P., LIU, H., YIN, H. & LI, H. 2012. Magnetotactic bacteria, magnetosomes and their application. *Microbiological Research,* 167**,** 507-519.

YU, B., YANG, M., SHI, L., YAO, Y., JIANG, Q., LI, X., TANG, L.-H., ZHENG, B.-J., YUEN, K.-Y., SMITH, D. K., SONG, E. & HUANG, J.-D. 2012a. Explicit hypoxia targeting with tumor suppression by creating an “obligate” anaerobic Salmonella Typhimurium strain. *Scientific Reports,* 2**,** 436.

YU, Y., GUTIERREZ, E., KOVACEVIC, Z., SALETTA, F., OBEIDY, P., RAHMANTO, Y. S. & RICHARDSON, D. R. 2012b. Iron Chelators for the Treatment of Cancer. *Current Medicinal Chemistry,* 19**,** 2689-2702.

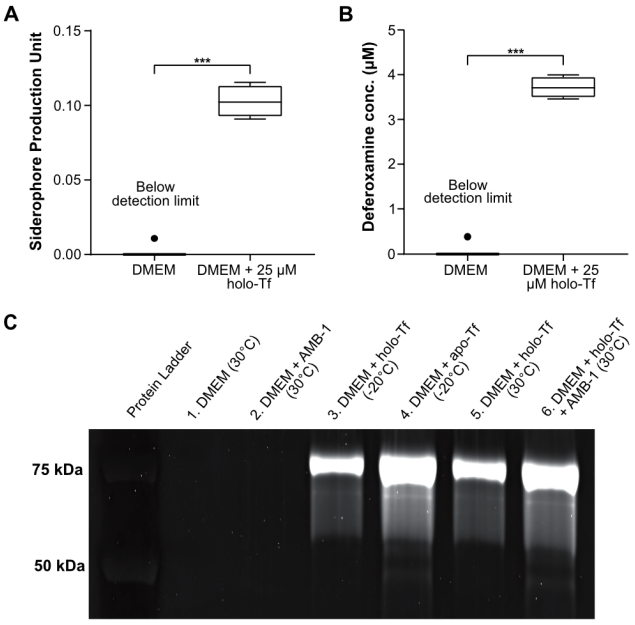

Figure 1: Quantification of siderophores produced by *Magnetospirillum magneticum* AMB-1 and analysis of their interaction with human transferrin. **(A)** Siderophores produced by AMB-1 were quantified by a chrome azurol S (CAS) assay in DMEM and DMEM supplemented with 25 µM holo-transferrin (n=4 per group, statistical significance was assessed with an unpaired two-tailed *t*-test). **(B)** Siderophore production units plotted in terms of the inferred equivalent concentration of deferoxamine (n=4 per group, statistical significance was assessed with an unpaired two-tailed *t*-test). **(C)** SDS-PAGE analysis displaying the effect of AMB-1 on the structure of human transferrin. Tested conditions are indicated in the figure, with holo-Tf corresponding to saturated transferrin and apo-Tf corresponding to non-saturated transferrin.

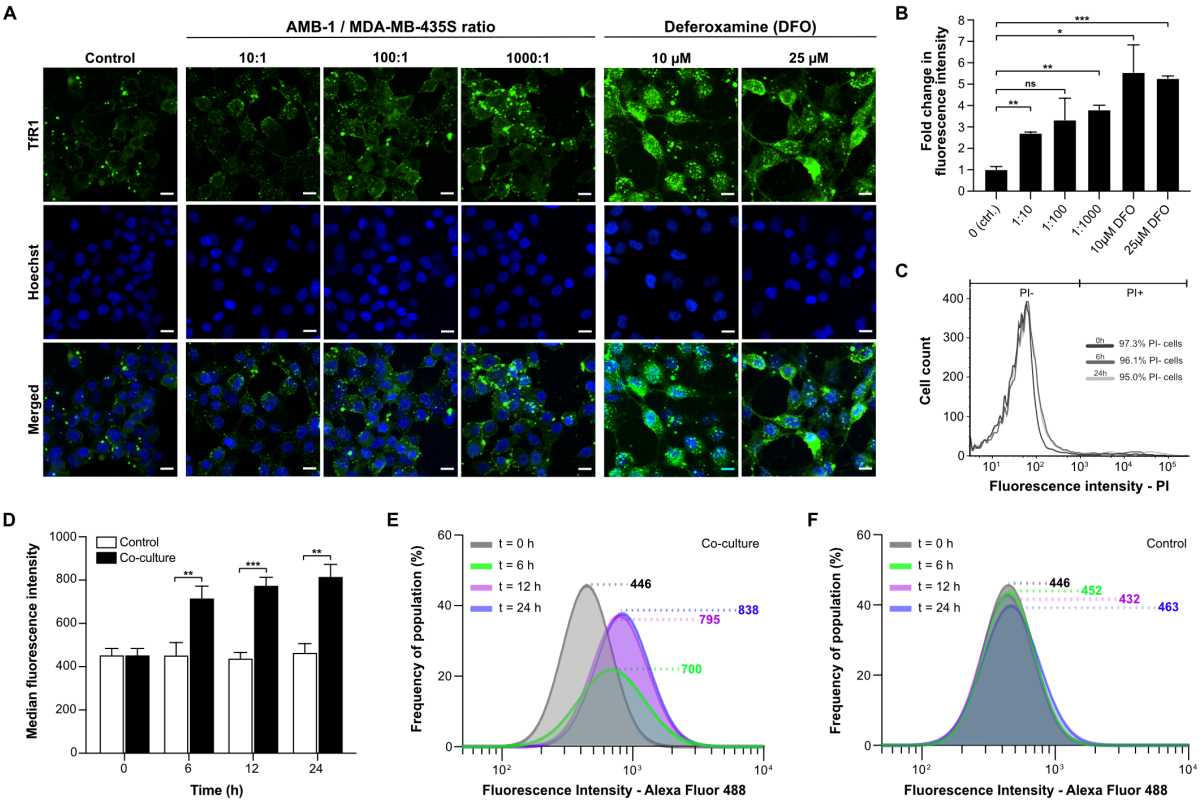

Figure 2: Analysis of TfR1 upregulation and cell surface expression on MDA-MB-435S. **(A)** Representative immunofluorescence images of human melanoma cells co-cultured under hypoxic conditions for 48 h with different ratios of AMB-1 bacteria and different concentrations of deferoxamine as a positive control. Images show MDA-MB-435S cells marked by anti-TfR1 antibody (green) and Hoechst 33342 (blue), (scale bar: 10 µM). **(B)** Quantification of the fold change in fluorescence intensity relative to the control condition, (n=2 per condition, statistical significance was assessed with an unpaired two-tailed *t*-test). **(C)** Membrane integrity was measured as a graphical representation of PI negative and PI positive cell populations after 0, 6 and 24 h. **(D)** TfR1 median fluorescence intensity measured over 24 hours, (n=3 per timepoint, statistical significance was assessed with an unpaired two-tailed *t*-test). **(E)** Representative log-normal fitted fluorescence intensity histograms of cell surface TfR1 expression on MDA-MB-435S cells in co-culture model and **(F)** negative control, (n=3 per timepoint).